

Effects of *Panax notoginseng* Saponin on Neurons Based on Oxygen-Glucose Deprivation/Reoxygenation after Focal Cerebral Ischemia

RILE WU*, QIANG YUN, JIANPING ZHANG AND JINGANG BAO

Department of Neurosurgery, Inner Mongolia People's Hospital, Saihan, Hohhot, Inner Mongolia Autonomous Region 010017, China

Wu et al.: *Panax notoginseng* Saponin and Neuroprotection

We aimed to evaluate the effects of *Panax notoginseng* saponin on neuronal apoptosis and neuroprotection based on oxygen-glucose deprivation/reoxygenation in rats with focal cerebral ischemia. 100 rats were randomly divided into sham operation, middle cerebral artery occlusion model, low-dose *Panax notoginseng* saponin (10 mg/kg), medium-dose *Panax notoginseng* saponin (25 mg/kg) and high-dose *Panax notoginseng* saponin (50 mg/kg) groups. The model of focal cerebral ischemia was established by middle cerebral artery occlusion. For sham group, the right common, external and internal carotid arteries were only dissociated, without ligation or insertion. After modeling, *Panax notoginseng* saponin groups were intraperitoneally injected with *Panax notoginseng* saponin. Hippocampal neurons isolated from normal rats were randomly divided into control, oxygen-glucose deprivation/reoxygenation model, 1 $\mu\text{mol/l}$, 5 $\mu\text{mol/l}$ and 20 $\mu\text{mol/l}$ oxygen-glucose deprivation/reoxygenation+*Panax notoginseng* saponin groups. Neurological function was scored by Longa method and neuron morphology was observed. Neuronuclear antigen and neuroepithelial stem protein in brain tissues were detected by immunohistochemistry. The survival rate of neurons, lactate dehydrogenase leakage, neuronal apoptosis and expression levels of protein kinase B, phosphorylated-protein kinase B and apoptosis-related proteins B-cell lymphoma 2, Bcl-2-associated X protein and caspase-3 were examined by cell counting kit-8 assay, lactate dehydrogenase kit, Hoechst 33 342 staining and Western blotting, respectively. Compared with model group, *Panax notoginseng* saponin groups had significantly lower neurological function scores ($p < 0.05$). *Panax notoginseng* saponin significantly relieved neuronal injury and increased neuronuclear and neuroepithelial stem protein-positive cells ($p < 0.05$). It significantly raised the survival rate of neurons, reduced lactate dehydrogenase leakage and inhibited neuronal apoptosis dose-dependently. *Panax notoginseng* saponin up-regulated the protein expressions of phosphorylated-protein kinase B/protein kinase B and B-cell lymphoma 2 and down-regulated those of Bcl-2-associated X protein and caspase-3 dose-dependently. It can protect against and repair neuronal injury caused by oxygen-glucose deprivation/reoxygenation, probably by activating the phosphatidylinositol 3-kinase/protein kinase B signaling pathway to suppress neuronal apoptosis.

Key words: *Panax notoginseng* saponin, hypoxia/ischemia, reperfusion, neuronal damage, apoptosis

Ischemic Cerebrovascular Diseases (ICVDs) are acute conditions characterized by high morbidity, disability and mortality rates, which are the third leading cause of human death, with the highest disability rate. Among them, ischemic stroke accounts for 80 % of global stroke cases^[1] and Cerebral Ischemia-Reperfusion Injury (CIRI) is the most harmful to the human body^[2]. In recent years, researchers have endeavored to determine different components in the brain using the specific markers of mature neurons, such as Neuronuclear (NeuN) antigen^[3], Glial Fibrillary Acidic Protein (GFAP)^[4] and Laminin (LN)^[5]. Ischemic injury involves many components in brain tissues that damage gray matter neurons, astrocytes, microglial

cells (supporting structures of neurons), nerve axons transmitting nerve signals and microvessels supplying oxygen and nutrients to neurons^[6].

Panax notoginseng saponin (PNS) is an effective active component of *Panax notoginseng*, which contains ginsenoside Rb1, ginsenoside Rb2 and notoginsenoside R₁^[7]. It is a natural estrogen receptor agonist with many protective effects such as anti-apoptotic, anti-

This is an open access article distributed under the terms of the Creative Commons Attribution-NonCommercial-ShareAlike 3.0 License, which allows others to remix, tweak, and build upon the work non-commercially, as long as the author is credited and the new creations are licensed under the identical terms

*Address for correspondence

E-mail: wurile@hotmail.com

Accepted 13 June 2022

Revised 14 August 2021

Received 18 January 2021

Indian J Pharm Sci 2022;84(3):740-749

inflammatory, anti-oxidative and anti-endoplasmic reticulum stress^[8]. PNS has been successfully applied in the clinical treatment of cerebral infarction in recent years^[9]. It can inhibit calcium overload and improve cerebral blood flow after ischemia, thus alleviating neuronal damage, promoting glial cell repair, protecting vascular endothelial cells and maintaining the integrity of endothelial barrier^[10]. Si *et al.* found that PNS was able to facilitate the proliferation and differentiation of hippocampal neural stem cells after ischemic brain injury in rats^[11]. Additionally, Li *et al.* confirmed that notoginsenoside R₁ in PNS alleviated the inflammatory reaction after ischemia-reperfusion, reduced intestinal microvascular permeability, protected vascular endothelial cells and maintained the integrity of intradermal barrier^[12].

In this study, therefore, an *in vitro* model of Oxygen-Glucose Deprivation/Reoxygenation (OGD/R) was established to investigate the protective effect of PNS on neurons. Besides, the protective effect of PNS on neuronal apoptosis and its regulatory effect on the Phosphoinositide 3 Kinase (P13K)/protein kinase B (Akt) signaling pathway were explored and the molecular mechanism of PNS for treating ICVDs was investigated, aiming to provide a theoretical basis for the clinical prevention of ischemic diseases with PNS.

MATERIALS AND METHODS

Ethical approval:

Ethical approval was sought and received from Inner Mongolia People's Hospital, China. The protocols for the use of animals in scientific research were strictly adhered to in compliance with the World Health Organization's provisions.

Experimental animals:

A total of 100 male Sprague-Dawley (SD) rats (Animal License No.: SCXK (Hunan) 2013-0002) aged 5-6 w old, with the body weight of 230-250 g (average body weight of (241.3±8.9) g), were purchased from Hunan SJA Laboratory Animal Co., Ltd. All animals were fed in our hospital at 21°-25° with the relative humidity of 50 %-60 % and natural illumination. They had free access to food and water in a clean feeding environment. After adaptive feeding for 1 w, experimental grouping and modeling were carried out.

Main reagents:

Materials included PNS (Shanghai Winherb Medical Technology Co., Ltd.), Dulbecco's Modified Eagle's

Medium (DMEM), fetal bovine serum (Gibco, USA), rabbit anti-mouse antibodies against polyclonal NeuN and polyclonal Neuroepithelial Stem Protein (Nestin) (Proteintech Group, Inc.), primary antibodies against pro-apoptosis proteins, including B-cell lymphoma 2 (Bcl-2), Bcl-2-Associated X protein (BAX) and Cysteiny Aspartate Specific Proteinase-3 (caspase-3), Akt and phosphorylated Akt (p-Akt) (Santa Cruz), mouse anti-beta (β)-actin antibody (Sigma, USA), Bicinchoninic Acid (BCA) protein kit, Radioimmunoprecipitation Assay (RIPA) lysis buffer and high-sensitivity Enhanced Chemiluminescence (ECL) kits (Beyotime Biotechnology Co., Ltd.) and horseradish peroxidase-labeled secondary antibody (Abcam, USA).

Apparatus:

A multifunctional microplate reader (BioTek, USA), a Carbon dioxide (CO₂) thermostatic incubator (Thermo, USA), a gel imaging analysis system (Alpha, USA) and an inverted phase contrast microscope (Olympus, Japan) were used.

Experimental grouping and establishment of focal cerebral ischemia:

The 100 rats were randomly allocated into 5 groups, i.e. sham operation group (sham group), Middle Cerebral Artery Occlusion (MCAO) model group and low-dose PNS (10 mg/kg) group (PNS-L group), medium-dose PNS (25 mg/kg) group (PNS-M group) and high-dose PNS (50 mg/kg) group (PNS-H group) (n=20). Next, the model of focal cerebral ischemia caused by MCAO was established according to the method specified previously^[13]. Model and PNS groups were anesthetized by intraperitoneal injection of 10 % chloral hydrate (0.35 g/kg). After a 3 cm incision was made in the middle of the front of the neck, the right common carotid artery, external carotid artery and internal carotid artery were bluntly dissected. The distal end of the external carotid artery was ligated with 5-0 surgical sutures and the artery and its branches proximal to the ligation point were coagulated and severed. Meanwhile, the distal side of the internal carotid artery was subjected to slip knot ligation. Then the distal side of the internal carotid artery and right common carotid artery were clamped with an artery clamp and the occlusion thread with a diameter of 0.28 mm was inserted into the internal carotid artery from the external carotid artery through the furcation between common and internal carotid arteries. Afterwards, the thread was inserted into the intracranial segment of internal carotid artery

for about (18±2) mm until the middle cerebral artery ring and tightened to prevent bleeding and movement. Subsequently, the neck skin was sutured layer by layer. After 2 h of ischemia, the occlusion thread was slowly pulled out for reperfusion. For the sham group, the right common carotid artery, external carotid artery and internal carotid artery were only dissociated, without ligation or insertion, and other operations were the same as those for MCAO model group.

Scoring of neurological function and administration:

The rats basically woke up 3-4 h after operation and their neurobehavioral function was scored based on the Longa scoring standard using 5-mark system^[14]. 0 points is without neurological deficits; 1 point for left forelimb flexion; 2 points for spontaneous left circling; 3 points for falling to the left and 4 points for without spontaneous movement or loss of consciousness. A higher score means severer neurological damage. The rats with scores of 1-3 points were regarded as successfully modeled and then used. PNS groups were intraperitoneally injected with different concentrations of PNS once a day until the end of the experiment. In the meantime, model and sham groups were injected with the same amount of normal saline. Twenty rats from each group were subjected to neurological function evaluation.

Observation of morphology of brain tissues:

Eight rats from each group were tested. The rats were anesthetized by intraperitoneal injection of 10 % chloral hydrate (0.35 g/kg) and decapitated, and their brains were collected. After removal of the olfactory bulb, cerebellum and lower brainstem, the brain tissues were fixed with 4 % paraformaldehyde. Afterwards, the brain tissues were cut into sections through coronal incision at the visual intersection plane. Following dehydration with gradient concentrations of ethanol solutions, transparentization using xylene and paraffin embedding, the tissues were cut into 4 µm thick serial sections. Immediately after Hematoxylin Eosin (HE) staining, 5 optical fields were taken from the ischemic cortex. The total number of cells and number of injured cells were observed under a microscope and the cell injury rate was calculated as follows:

Cell injury rate (%)=(Number of injured cells/Total number of cells)×100 %

Detection of Nestin and NeuN protein expressions by immunohistochemistry:

Eight rats from each group were tested. After deep anesthesia, the brain tissues were harvested and the specimens were fixed with 4 % paraformaldehyde solution. Then they were embedded in paraffin, frozen at -20° for 2 h, cut into 4 µm thick serial sections, baked in an oven at 75° for 1 h and cooled at room temperature. Next, the sections were deparaffinized with xylene, hydrated with gradient concentrations of ethanol solutions, washed by Phosphate-Buffered Saline (PBS) and dripped with 3 % hydrogen peroxide-methanol to remove endogenous peroxidase. Later, the sections were added with citric acid antigen retrieval solution and heated for 20 min. Afterwards, the sections were added with anti-Nestin polyclonal antibody and anti-NeuN monoclonal antibody diluted at 1:1500 drop wise and incubated with primary antibodies at 4° overnight. On the next day, goat anti-mouse Immunoglobulin G (IgG) labeled with horseradish peroxidase was added, followed by HE staining. Under the microscope, positively expressed neurons were brown granules. Nestin was mainly expressed in the cytoplasm, and NeuN was primarily expressed in the nucleus and cytoplasm of neurons. Five optical fields were taken from each section and the number of positive cells in each field was calculated.

Positive cell rate (%)=(Number of positive cells/Total number of cells)×100 %

Isolation and culture of hippocampal neurons:

Four normal rats were tested. After the rats were killed under deep anesthesia, their cerebral cortex was isolated on a sterile clean bench and the hippocampus was separated under a dissecting microscope and placed in precooled D-Hank's solution. After the tissues were cut into small pieces, they were digested with 0.25 % trypsin at 37° for 8 min and digestion was terminated with high-glucose DMEM containing 10 % fetal bovine serum. Later, the tissues were filtered with a 200-mesh copper mesh and centrifuged for 5 min (1000 r/min). The separated cells were resuspended in neurobasal (2 % B27) culture medium and inoculated in a culture bottle pre-coated with poly-L-lysine (100 mg/l). Finally, the cells were placed in a thermostatic incubator for passage at 37° with 5 % CO₂ and saturated humidity for 7 d, and the medium was replaced once every 2-3 d.

OGD/R grouping of neurons and model establishment:

Hippocampal neural stem cells cultured for 7 d were randomly allocated into control, OGD/R and OGD/R+PNS (1, 5, 20 µmol/l) groups. Control group was

incubated in glucose-free neurobasal solution for 48 h, OGD/R group was treated with OGD for 4 h and incubated in the thermostatic incubator for 48 h, and OGD/R+PNS groups were inoculated into glucose-free neurobasal solution containing PNS (15 µg/ml) and treated in the same way as the OGD/R group.

Detection of neuronal survival rate:

The cell viability was detected using Cell Counting Kit-8 (CCK-8) assay. The cells in the logarithmic growth phase were inoculated in 96-well plates at 5×10^4 /ml for 24 h and then an OGD/R model was established. After 4 h of reoxygenation, 10 µl of CCK-8 was added to each well. Following incubation in the thermostatic incubator for 3 h, the absorbance (570 nm) of each well was measured using the microplate reader and the relative survival rate was calculated by converting the absorbance ratio^[15].

Detection of neuronal Lactate Dehydrogenase (LDH):

After the cells were reoxygenated for 24 h, the supernatant was collected and the LDH level was determined according to the instructions of LDH kit.

Detection of neuronal apoptosis:

The neural stem cells were inoculated into 96-well culture plates at a density of 6×10^4 /ml. After OGD/R for 24 h, the supernatant was discarded and the cells were washed with PBS and fixed by 4 % paraformaldehyde. After washing with PBS again, the cells were stained by Hoechst 33 342/Propidium iodide (PI) working solution and incubated at 4° for 30 min in dark. Later, the working solution was sucked out and the cells were washed with PBS. After mounting with glycerol, the fluorescence intensity was observed under an inverted fluorescence microscope.

Detection of protein expressions by Western blotting:

The cells were collected, lysed in RIPA lysis buffer with phosphatase inhibitors and protease inhibitors for 30 min on ice and centrifuged for 10 min (12 500 r/min) using a refrigerated centrifuge. After the supernatant was collected, the protein concentration was detected by BCA method and total protein was subjected to Sodium Dodecyl-Sulfate Polyacrylamide Gel Electrophoresis (SDS-PAGE) (5 % stacking gel+10 % separation gel, 80 V, 100 min). Next, the protein was transferred onto a Polyvinylidene Difluoride (PVDF) membrane that

was then washed by Tris-Buffered Saline (TBS) for 10 min, diluted with 5 % blocked protein dry powder diluent and blocked for 2 h. Later, the membrane was incubated with primary antibodies against BAX, Bcl-2, caspase-3, Akt and p-Akt at 4° overnight and with the corresponding secondary antibodies for 1-2 h on the next day. Following ECL color development, ImageJ2x imaging system was utilized to analyze the gray values of protein bands.

Statistical analysis:

Statistical Package for the Social Sciences (SPSS) 18.0 software was used for statistical analysis. One-way analysis of variance was applied to analyze the differences between groups. $p < 0.05$ indicated that the differences were statistically significant and GraphPad Prism5.0 software was used for plotting.

RESULTS AND DISCUSSION

Compared with sham group, the neurological function score of MCAO model group significantly increased ($p < 0.01$). In comparison with MCAO model group, PNS groups had significantly lower neurological function scores ($p < 0.05$, $p < 0.01$) as shown in fig. 1.

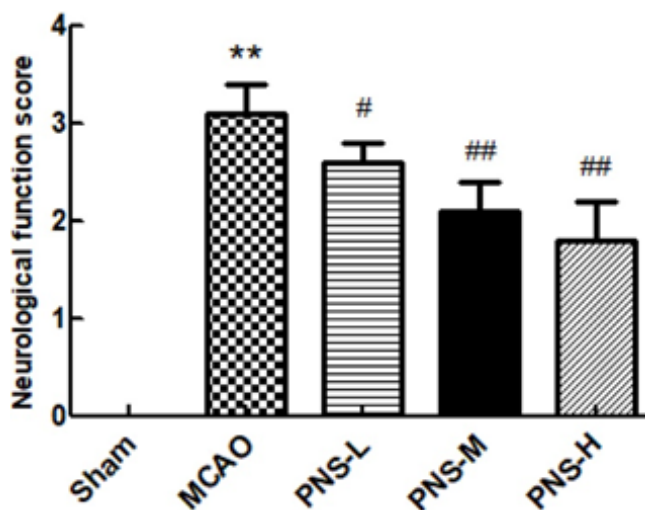


Fig. 1: Neurological function scores

Note: ** $p < 0.01$ vs. sham group and # $p < 0.05$; ## $p < 0.01$ vs. MCAO model group

The brain tissue structure in the cortical area was complete, closely connected and regular in shape, the nucleolus was clearly visible and the cell damage was mild in sham group. In MCAO model group, the intercellular substance in the cortical area was obviously oedematous, the nucleus was irregular, cells were disordered and nuclear pyknosis or acidophilic degeneration occurred. Compared with sham group, the number of injured cells and the cell injury rate increased

significantly in MCAO model group ($p < 0.01$). After PNS intervention, the injury degree and rate of cortical cells reduced ($p < 0.05$, $p < 0.01$), the edema of cells was relieved and the tissue structure tended to be complete as shown in fig. 2 and fig. 3.

In control group, the number of NeuN-positive cells was larger, while that of Nestin-positive cells was smaller in the hippocampus. MCAO group had significantly fewer NeuN-positive cells and more Nestin-positive cells than those of sham group ($p < 0.01$). In comparison with MCAO model group, the number of NeuN and Nestin positive cells in PNS group increased significantly ($p < 0.05$) as shown in fig. 4-fig. 6. After 4 h of reoxygenation, the absorbance of cells was measured at 570 nm. Compared with control group, the survival rate of neurons in OGD/R model group significantly declined ($p < 0.01$). After PNS treatment, the survival rate of neurons was raised significantly in a concentration-dependent manner compared with that of OGD/R model group. Besides, the survival rates of PNS-M and

PNS-L groups were significantly different from that of OGD/R model group ($p < 0.05$, $p < 0.01$), indicating that PNS pretreatment elevated the survival rate of OGD/R-injured neurons as shown in fig. 7. Compared with control group, the LDH leakage of neurons in OGD/R model group rose significantly ($p < 0.01$) and significantly dropped in PNS group compared with that in OGD/R model group. In addition, the leakages of PNS-M and PNS-L groups were significantly different from that of model group ($p < 0.05$, $p < 0.01$) suggesting that PNS reduced the LDH leakage of OGD/R-injured neurons and protected the cell membranes as shown in fig. 8. After Hoechst 33 342/PI double staining, normal cells showed weak blue+low red fluorescence, while apoptotic cells showed strong blue+low red fluorescence. Compared with sham group, OGD/R model group showed strong blue+low red fluorescence and the intensity increased significantly but decreased after PNS intervention, indicating that PNS suppressed neuronal apoptosis caused by OGD/R injury as shown in fig. 9.

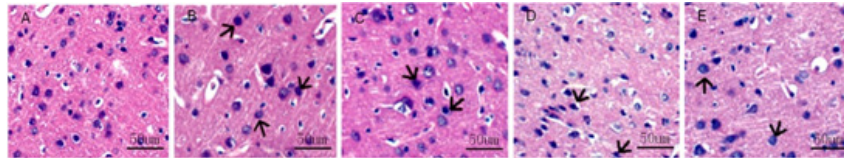


Fig. 2: Pathological changes in the cortex (magnification: 400 \times), (A): Sham group; (B): MCAO model group; (C): PNS-L group; (D): PNS-M group and (E): PNS-H group

Note: The cells with nuclei deeply stained with pyknosis or acidophilic degeneration indicated by arrows were damaged cells

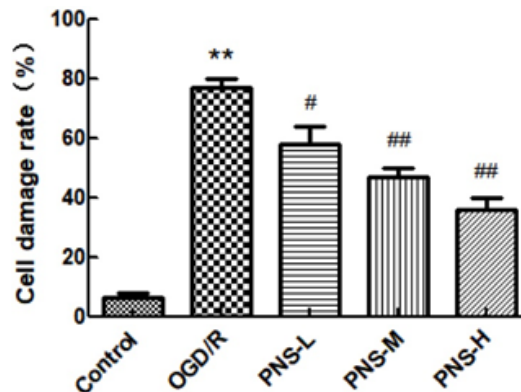


Fig. 3: Cell injury rates

Note: ** $p < 0.01$ vs. sham group and # $p < 0.05$; ## $p < 0.01$ vs. MCAO model group

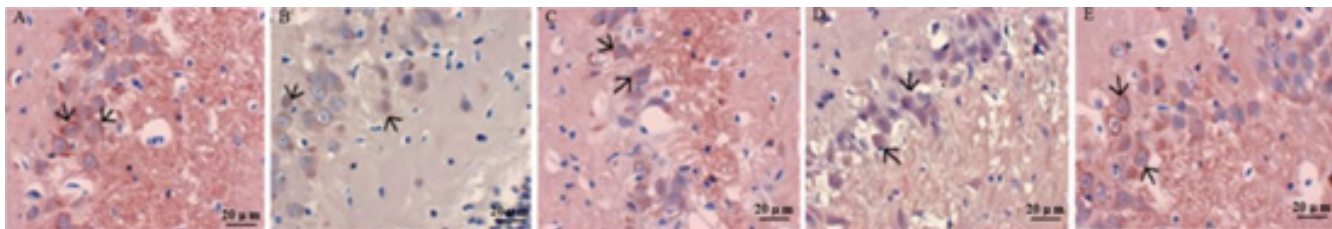


Fig. 4: NeuN staining results in the hippocampal CA1 region, (A): Sham group; (B): MCAO model group; (C): PNS-L group; (D): PNS-M group and (E): PNS-H group

Note: Arrow: Positive expression of protein

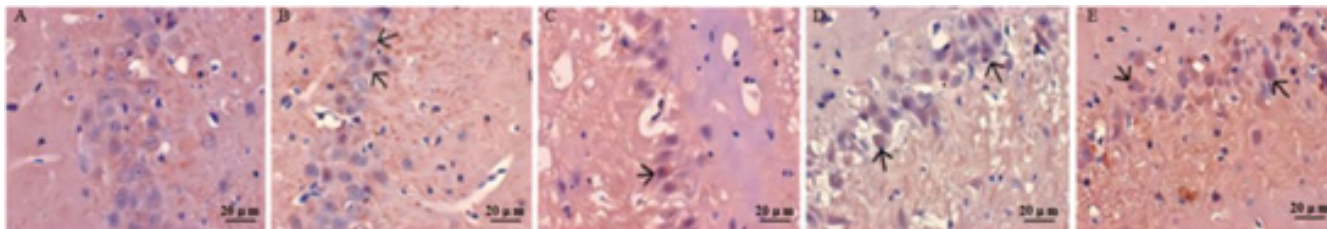


Fig. 5: Nestin staining results in the hippocampal CA1 region, (A): Sham group; (B): MCAO model group; (C): PNS-L group; (D): PNS-M group and (E): PNS-H group

Note: Arrow: Positive expression of protein

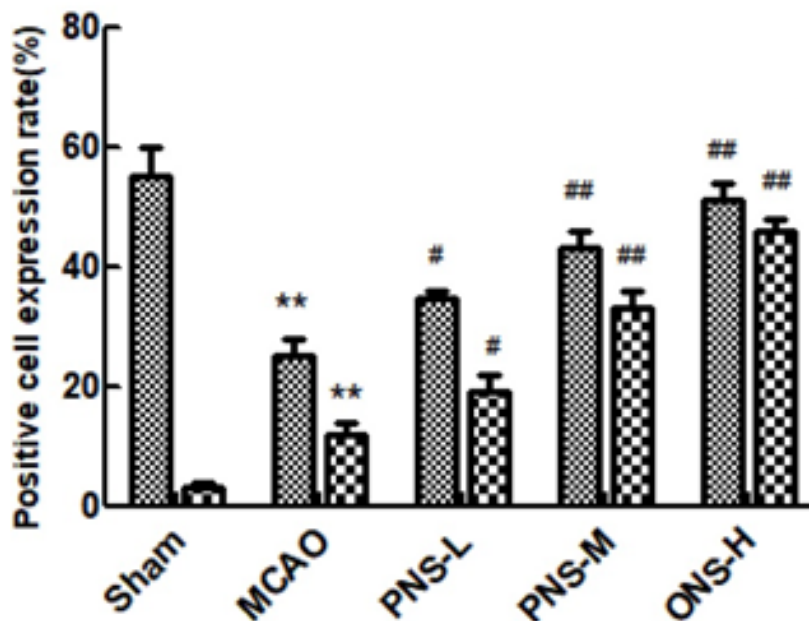


Fig. 6: Protein expressions of NeuN and Nestin in the hippocampal CA1 region

Note: **p<0.01 vs. sham group and #p<0.05; ##p<0.01 vs. MCAO model group, (▨): NeuN and (▩): Nestin

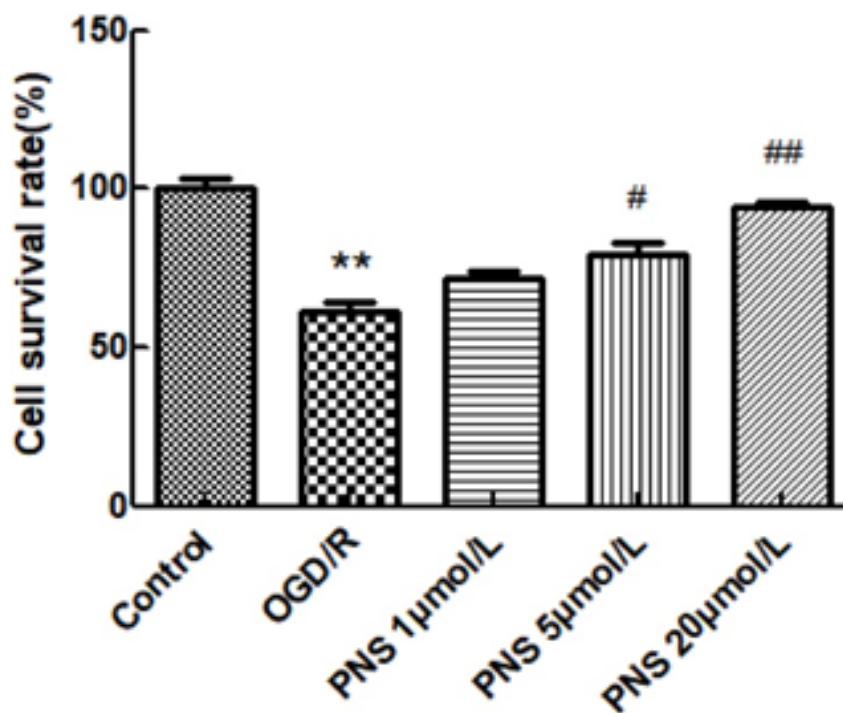


Fig. 7: Effects of PNS on survival rates of OGD/R-injured neurons

Note: **p<0.01 vs. control group and #p<0.05, ##p<0.01 vs. OGD/R model group

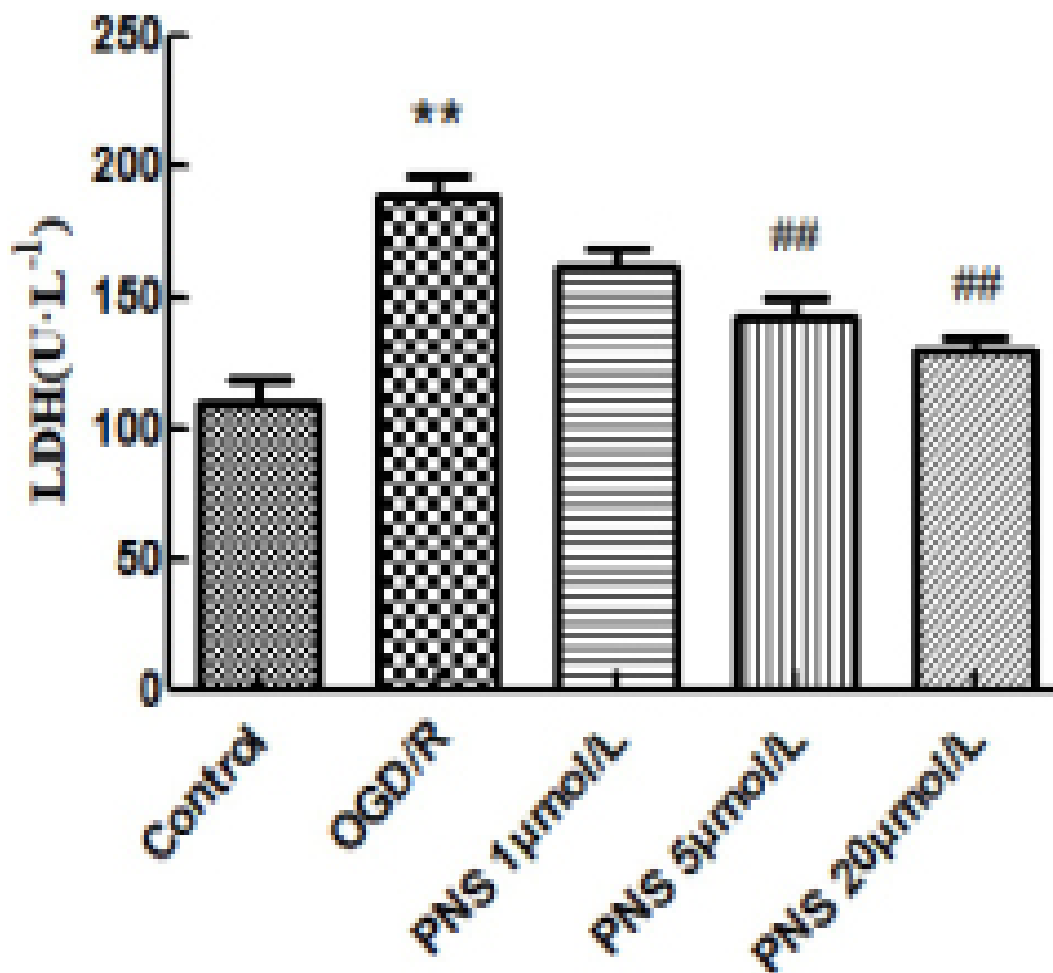


Fig. 8: Effects of PNS on LDH leakage of OGD/R-injured neurons

Note: ** $p < 0.01$ vs. control group and # $p < 0.05$; ## $p < 0.01$ vs. OGD/R model group

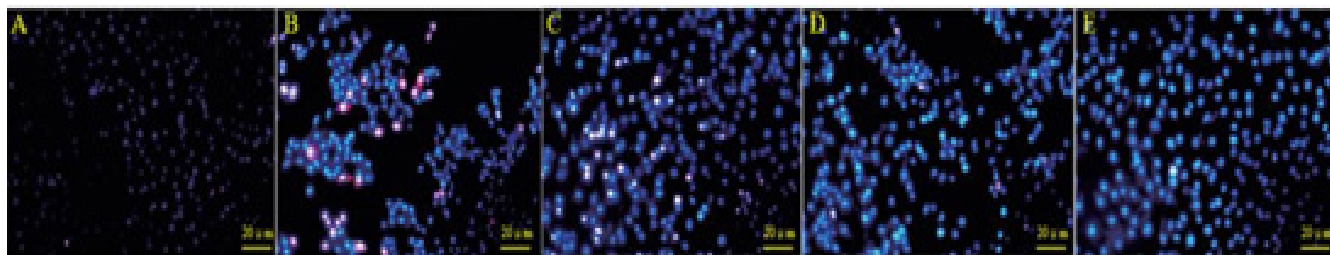


Fig. 9: Effects of PNS on apoptosis of neurons injured by OGD/R, (A): Control group; (B): OGD/R model group; (C): OGD/R+PNS (1 µmol/l) group; (D): OGD/R+PNS (5 µmol/l) group and (E): OGD/R+PNS (20 µmol/l) group

The protein expressions of Bcl-2, BAX and caspase-3 were detected by Western blotting. In comparison with control group, the protein expression of Bcl-2 in OGD/R model group declined, while those of BAX and caspase-3 rose significantly ($p < 0.05$). Compared to OGD/R model group, OGD/R+PNS groups had elevated protein expression of Bcl-2 but significantly reduced protein expressions of BAX and caspase-3 ($p < 0.05$). Collectively, PNS can down-regulate the protein expressions of BAX and caspase-3 and up-regulate that of Bcl-2 in neurons injured by OGD/R as

shown in fig. 10.

In comparison with control group, the protein expression of p-Akt/Akt in OGD/R model group dropped significantly ($p < 0.05$). Compared with OGD/R model group, PNS groups had increased protein expression of p-Akt/Akt in a concentration-dependent manner ($p < 0.05$), implying that PNS activated the Phosphatidylinositol 3-Kinase (PI3K)/Akt signaling pathway of neurons injured by OGD/R as shown in fig. 11.

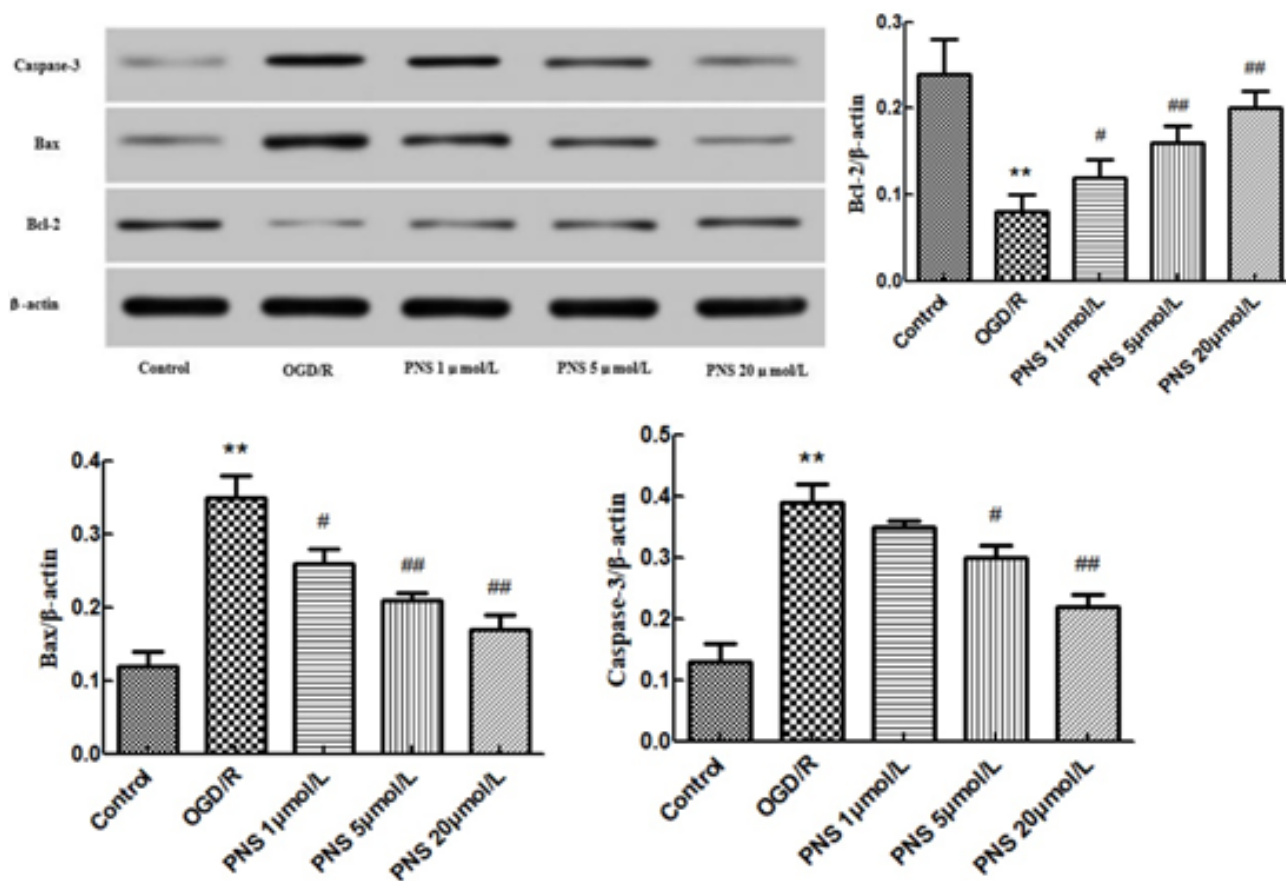


Fig. 10: Effects of PNS on protein expressions of Bcl-2, BAX and caspase-3 in neurons injured by OGD/R

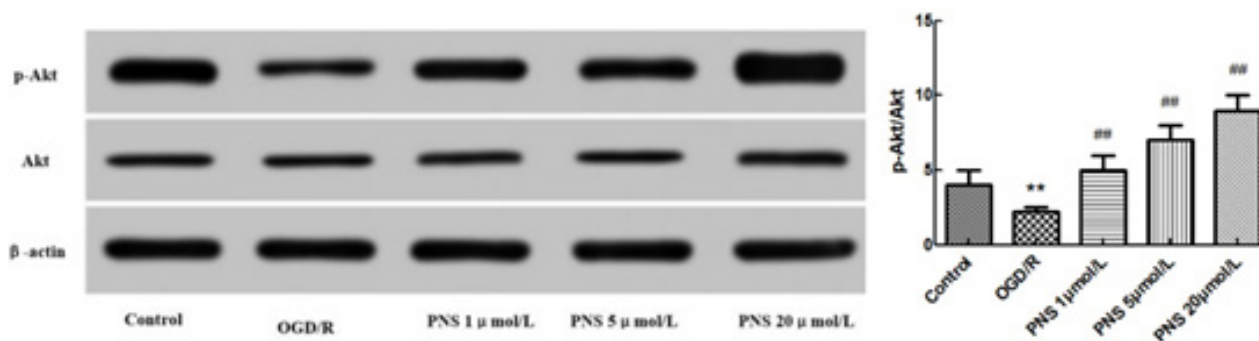


Fig. 11: Effects of PNS on protein expressions of p-Akt/Akt in neurons injured by OGD/R

CIRI participates in and interacts with each other through various mechanisms, which leads to edema, degeneration and necrosis of brain cells in the ischemic area, necrosis or apoptosis of endothelial cells, changes of cerebrovascular structure and destruction of blood-brain barrier function after cerebral ischemia-reperfusion, thus forming cerebral infarction foci and eventually causing cerebral dysfunction^[16]. Apoptosis after CIRI is the main form of neuronal death^[17], so finding anti-neuronal apoptosis drugs is of great significance to the repair of CIRI. PNS is a main effective component of *Panax notoginseng*, which can improve cerebral microcirculation after ischemia, dilate blood

vessels, resist inflammation and oxidation, scavenge free radicals, protect endothelial cells, promote their regeneration and inhibit apoptosis^[18].

In this study, PNS markedly reduced the neurological function score of rats and alleviated the cell injury in the cerebral cortex, indicating that PNS mitigated the neurological dysfunction of CIRI rats. NeuN is a specific marker of mature neurons^[19] and the up-regulation of NeuN protein expression can reflect the maturity of neurons. Cerebral ischemia and hypoxia result in neuronal injury and death. Nestin is a neural stem cell-specific marker protein. There are only a few

Nestin-positive cells in the hippocampus of normal adult rats. After ischemic brain injury, the Nestin-positive cells in the Stratum Griseum Centrale (SGC) and Subventricular Zone (SVZ) regions of hippocampal dentate gyrus increase, suggesting that ischemic brain injury can induce the proliferation and differentiation of endogenous neural stem cells^[20]. Herein, after the modeling of focal cerebral ischemia, the expression of NeuN declined dramatically and the positive expression of Nestin increased in the hippocampus of rats, implying that focal cerebral ischemia inhibited the differentiation of neurons and induced the proliferation and repair of neurons. Moreover, PNS intervention notably raised the protein expressions of NeuN and Nestin in the hippocampus, indicating that PNS facilitated the proliferation, differentiation and maturation of neurons after ischemia-reperfusion.

In this study, the cortical neurons of SD rats were cultured *in vitro*, and the OGD/R model was established to simulate the neuronal injury caused by cerebral ischemia and to explore the neuroprotective effect of PNS. Based on the PI3K/Akt signaling pathway, the molecular mechanism of PNS against OGD/R-injured neuronal apoptosis was explored. PNS evidently increased the survival rate of neurons, reduced LDH leakage and inhibited neuronal apoptosis, suggesting that PNS exerted an obvious neuroprotective effect, which is consistent with a previous literature^[20]. After intracerebral hemorrhage, the neurons around hematoma suffered from ischemia and hypoxia due to the compression of hemorrhage focus and secreted apoptotic factors of neurons, thus triggering neuronal apoptosis. Bcl-2, BAX and caspase-3 are considered as vital regulatory genes that inhibit or promote apoptosis^[21]. Furthermore, we herein found that PNS down-regulated the protein expressions of BAX and caspase-3 and up-regulated that of Bcl-2 in OGD/R-injured neurons. Thus, PNS protects OGD/R-injured neurons by regulating apoptosis-related genes.

The PI3K/Akt signaling pathway, which is crucial for cell survival, exerts a pivotal effect on regulating neuronal apoptosis after cerebral ischemia, as a key transduction pathway for cell metabolism and anti-apoptosis^[22]. The Bcl-2 protein family is composed of anti-apoptotic (Bcl-2, B-cell lymphoma-Extra-Large (Bcl-XL), etc.) and pro-apoptotic proteins BAX, Bcl-associated killer (Bak), etc., which are the downstream executive proteins of the PI3K/Akt signaling pathway. After cerebral ischemia, PI3K can be activated, inducing the phosphorylation of Akt, phosphorylating

BCL2 associated Agonist of Cell Death (BAD) protein, inhibiting its binding with Bcl-2 and Bcl-XL, and increasing the protein expressions of free Bcl-2 and Bcl-XL in the cytoplasm, thereby exerting an anti-apoptotic effect^[23]. Besides, p-Akt can inhibit apoptosis by suppressing the expressions of BAX-Bcl-2 dimer and caspase-3 protein. In the present study, the effects of PNS on the PI3K/Akt signaling pathway and apoptosis-related proteins in neurons injured by OGD/R were evaluated. The levels of p-Akt and Bcl-2 in neurons injured by OGD/R were significantly lower than those in control group, while the protein expressions of BAX and caspase-3 dramatically increased, suggesting that OGD/R injury suppressed the activation of the PI3K/Akt signaling pathway but enhances the phosphorylation level of Akt in OGD/R-injured neurons in a concentration-dependent manner. Hence, the neuroprotection of PNS may be related to its activation of the PI3K/Akt signaling pathway.

In summary, PNS can protect against and repair neuron injury caused by CIRI, probably by activating the PI3K/Akt signaling pathway to inhibit neuronal apoptosis.

Conflict of interests:

The authors declared no conflicts of interest.

REFERENCES

1. Fan J, Li Y, Fu X, Li L, Hao X, Li S. Nonhuman primate models of focal cerebral ischemia. *Neural Regen Res* 2017;12(2):321-8.
2. Stegner D, Klaus V, Nieswandt B. Platelets as modulators of cerebral ischemia/reperfusion injury. *Front Immunol* 2019;10:2505.
3. Sukhorukova EG. Nuclear protein NeuN in neurons in the human substantia nigra. *Neurosci Behav Physiol* 2014;44(5):539-41.
4. Rieske P, Azizi SA, Augelli B, Gaughan J, Krynska B. A population of human brain parenchymal cells expresses markers of glial, neuronal and early neural cells and differentiates into cells of neuronal and glial lineages. *Eur J Neurosci* 2007;25(1):31-7.
5. Bannerman PG, Mirsky R, Jessen KR. Antigenic markers and laminin expression in cultured enteric neural cells. *Brain Res* 1988;440(1):87-98.
6. Tanaka K. Pathophysiology of brain injury and targets of treatment in acute ischemic stroke. *Rinsho Shinkeigaku* 2013;53(11):1159-62.
7. Xie XS, Yang M, Liu HC, Zuo C, Li HJ, Fan JM. Ginsenoside Rg1, a major active component isolated from *Panax notoginseng*, restrains tubular epithelial to myofibroblast transition *in vitro*. *J Ethnopharmacol* 2009;122(1):35-41.
8. Wang MM, Xue M, Xu YG, Miao Y, Kou N, Yang L, et al. *Panax notoginseng* saponin is superior to aspirin in inhibiting platelet adhesion to injured endothelial cells through COX pathway *in vitro*. *Thromb Res* 2016;141:146-52.

9. Xu C, Wang W, Wang B, Zhang T, Cui X, Pu Y, *et al.* Analytical methods and biological activities of *Panax notoginseng* saponins: Recent trends. *J Ethnopharmacol* 2019;236:443-65.
 10. Wang S, Li M, Guo Y, Li C, Wu L, Zhou XF, *et al.* Effects of *Panax notoginseng* ginsenoside R_{b1} on abnormal hippocampal microenvironment in rats. *J Ethnopharmacol* 2017;202:138-46.
 11. Si YC, Zhang JP, Xie CE, Zhang LJ, Jiang XN. Effects of *Panax notoginseng* saponins on proliferation and differentiation of rat hippocampal neural stem cells. *The Am J Chin Med* 2011;39(5):999-1013.
 12. Li C, Li Q, Liu YY, Wang MX, Pan CS, Yan L, *et al.* Protective effects of notoginsenoside R₁ on intestinal ischemia-reperfusion injury in rats. *Am J Physiol Gastrointest Liver Physiol* 2014;306(2):G111-22.
 13. Xu D, Huang P, Yu Z, Xing DH, Ouyang S, Xing G. Efficacy and safety of *Panax notoginseng* saponin therapy for acute intracerebral hemorrhage, meta-analysis and mini review of potential mechanisms of action. *Front Neurol* 2015;5:274.
 14. Longa EZ, Weinstein PR, Carlson S, Cummins R. Reversible middle cerebral artery occlusion without craniectomy in rats. *Stroke* 1989;20(1):84-91.
 15. Li Y, Hu K, Liang M, Yan Q, Huang M, Jin L, *et al.* Stilbene glycoside up regulates SIRT3/AMPK to promotes neuronal mitochondrial autophagy and inhibit apoptosis in ischemic stroke. *Adv Clin Exp Med* 2021;30(2):139-46.
 16. Wang M, Li YJ, Ding Y, Zhang HN, Sun T, Zhang K, *et al.* Silibinin prevents autophagic cell death upon oxidative stress in cortical neurons and cerebral ischemia-reperfusion injury. *Mol Neurobiol* 2016;53(2):932-43.
 17. Liu B, Li F, Shi J, Yang D, Deng Y, Gong Q. Gastrodin ameliorates subacute phase cerebral ischemia reperfusion injury by inhibiting inflammation and apoptosis in rats. *Mol Med Rep* 2016;14(5):4144-52.
 18. Duan L, Xiong X, Hu J, Liu Y, Li J, Wang J. *Panax notoginseng* saponins for treating coronary artery disease: A functional and mechanistic overview. *Front Pharmacol* 2017;8:702.
 19. Gusel'Nikova VV, Korzhevskiy D. NeuN as a neuronal nuclear antigen and neuron differentiation marker. *Acta Naturae* 2015;7(2):42-7.
 20. Xiong LL, Qiu DL, Xiu GH, Al Hawwas M, Jiang Y, Wang YC, *et al.* DPYSL2 is a novel regulator for neural stem cell differentiation in rats: Revealed by *Panax notoginseng* saponin administration. *Stem Cell Res Ther* 2020;11(1):155.
 21. Liu G, Wang T, Wang T, Song J, Zhou Z. Effects of apoptosis related proteins caspase 3, BAX and Bcl 2 on cerebral ischemia rats. *Biomed Rep* 2013;1(6):861-7.
 22. Zhang QZ, Guo YD, Li HM, Wang RZ, Guo SG, Du YF. Protection against cerebral infarction by Withaferin A involves inhibition of neuronal apoptosis, activation of PI3K/Akt signaling pathway and reduced intimal hyperplasia *via* inhibition of VSMC migration and matrix metalloproteinases. *Adv Med Sci* 2017;62(1):186-92.
 23. Yu ZH, Cai M, Xiang J, Zhang ZN, Zhang JS, Song XL, *et al.* PI3K/Akt pathway contributes to neuroprotective effect of Tongxinluo against focal cerebral ischemia and reperfusion injury in rats. *J Ethnopharmacol* 2016;181:8-19.
-